Modeling Pitting Degradation of Corrosion Resistant Alloys

Gregory A. Henshall

November 1996

Modeling Pitting Degradation of Corrosion Resistant Alloys
Gregory A. Henshall

Lawrence Livermore National Laboratory
June 1996

Abstract

A computer model capable of simulating the time and environmental dependence of pit initiation, growth, and cessation of growth has been developed. This phenomenological model is capable of predicting the time required for initiation of pitting and the development of a "pitting damage function," *i.e.* the distribution of pit depths, for arbitrary environmental histories. The model is based on a stochastic approach of describing pit initiation and growth but includes some aspects of the deterministic features of pit growth.

Recent improvements to the model provide the capability to simulate permanent pit growth cessation and a decreasing time or depth dependence of pit growth rates. The results of example calculations demonstrate that these additions allow the model to simulate, in a physically meaningful way, the commonly reported evolution of asymmetric pit depth distributions and the nonlinear increase in maximum pit depth with increasing exposure time. An extreme-value statistical analysis also has been incorporated within the improved computer code, which allows it to predict a logarithmic increase in maximum pit depth with increasing surface area, as suggested by data and theory. This addition provides a method for extrapolating experimental pit depth data gathered using small laboratory samples to the very large container surface areas that would be exposed in the potential high level nuclear waste repository.

Unfortunately, the lack of experimental data from which to generate code input parameters for candidate waste package container materials in repository-relevant environments seriously handicaps the application of this code to performance assessment activities. Recently, a limited number of experiments have been performed on Alloy 825 in repository-relevant environments. Preliminary data for the pit depth distribution in potentiostatically-polarized Alloy 825 are presented and demonstrate the viability of generating data with which to compare model predictions. The need for additional experimental efforts is discussed.

TABLE OF CONTENTS

1. Introduction

1.1 Modeling pitting of waste package containers

A multiple barrier concept currently is being employed in the development of waste package (WP) containers for use in the potential geological repository for spent nuclear fuel and high level nuclear waste at Yucca Mountain, Nevada. Current WP development considers designs to enclose spent nuclear fuel from commercial power reactors in one design and reprocessed high-level borosilicate glass waste in another similar design. In either case, one of the barriers will be constructed of a highly corrosion resistant material, such as a Ni- or Ti-base alloy. Normally, such alloys are protected by a passive oxide film, but if they become wet and Cl^- or other aggressive species are present, the passive film can break down locally, causing localized corrosion. Of the three forms of localized corrosion[1], *viz*. pitting, crevice corrosion, and stress-corrosion cracking, that are likely to occur on WP surfaces exposed to repository environments, pitting corrosion was chosen for detailed modeling. Pitting corrosion was selected because it bears many similarities to crevice corrosion. Therefore, many aspects of the pitting model are expected to be directly applicable to the crevice corrosion model. It was decided to defer development of a validated model of stress-corrosion cracking until additional experimental information on the stress-corrosion behavior of candidate container materials under repository relevant-conditions becomes available.

Factors driving the development and experimental validation of a pitting corrosion model are centered around the need to understand the behavior of candidate waste container materials that may undergo localized corrosion in repository-relevant environments. The availability of such a model would minimize the risk of missing some critical interaction of material and environment that would result in premature failure of the container. The specific factors include:

1. A total lack of operational information on long-term storage of high-level nuclear waste;

2. Uncertainty and variability in the environmental conditions, and possible changes in these conditions;

3. The need to make technically defensible extrapolations to very long times based on experimental data bases developed over very short times (with respect to repository lifetimes); and

4. The need to make technically defensible extrapolations to very large exposed surface areas based on experimental data bases developed from much smaller areas.

1

In contrast to uniform corrosion, where mechanistic modeling has been successful, a statistical approach to characterizing and modeling localized corrosion appears to be necessary, even though the data requirements are large[2]. One advantage of a statistical, or stochastic, model is that the evolution of the pit depth *distribution*, not just the time required for initial penetration of the containers, can be computed. From this information the area available for release of radionuclides through the container walls can be estimated as a function of time[3]. This report describes a phenomenological approach for computing the time evolution of these distributions that is largely stochastic in nature but combines some elements of the deterministic aspects of pit growth.

The pit depth distribution, or pitting corrosion damage function, is illustrated schematically in Fig. 1. It is simply a plot of the number (or frequency) of pits at a particular depth *vs* depth. The damage function may be represented by smooth curves, as in Fig. 1, or as a series of histograms, as shown later in this report. From a modeling standpoint, the damage function is computed for various exposure times assuming that the metal being pitted is infinitely thick. These curves then can be compared with the actual wall thickness of the WP container, as shown in Fig. 1. The predicted time required for the first pit to penetrate the container wall is that at which the computed damage function first intersects the line corresponding to the wall thickness (t_2 in Fig. 1). At longer times, the *number* of pits penetrating the container wall is proportional to the area under the damage function curve for pit depths greater than the wall thickness (the shaded area under the t_3 curve). The calculated *depths* of through-wall pits have no physical significance, since a pit cannot have a depth greater than the wall thickness.
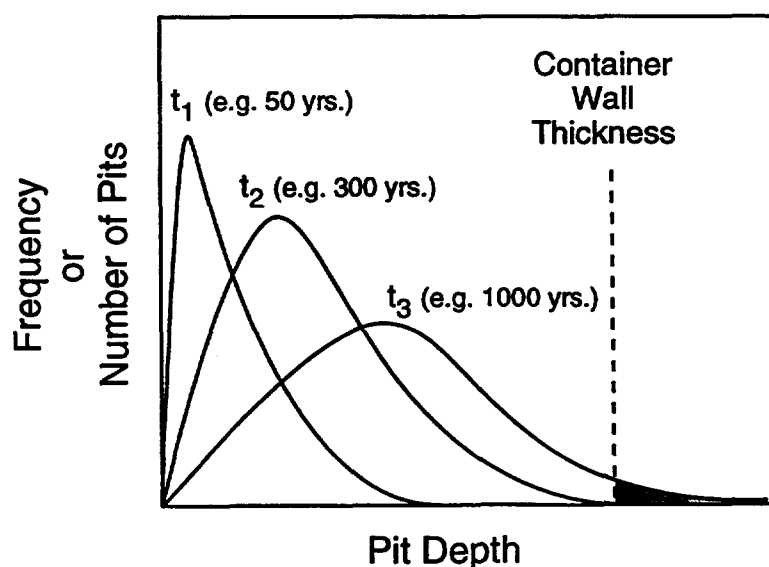
Figure 1. Schematic illustration of the pitting corrosion damage function.
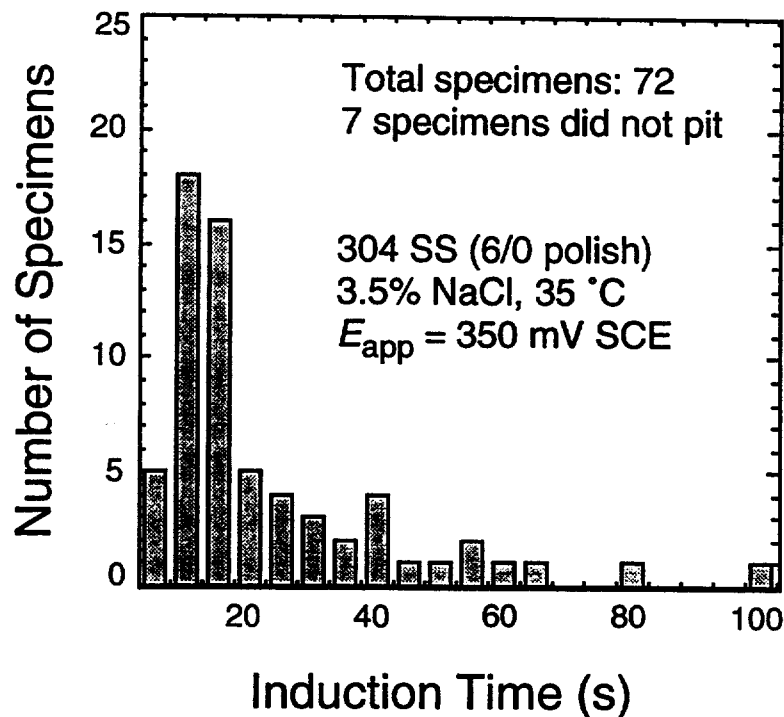
Figure 2. The induction time distribution for 72 identical Type 304 stainless steel specimens immersed in NaCl solution. Data of Shibata and Takeyama[4].

1.2 The stochastic nature of pitting corrosion

Experimental studies have shown that the initiation of corrosion pits is a stochastic process. Shibata and Takeyama[4] were the first to show that the critical potential necessary to induce pitting and the "induction" time elapsed before pits become observable are both statistically distributed quantities. For example, Fig. 2 presents their data showing the distribution of induction times for 72 ostensibly identical Type 304 stainless steel specimens subjected to identical conditions. The data exhibit a wide distribution of induction times, suggesting that pit initiation occurs stochastically.

There is also evidence that the growth of existing pits is a stochastic process. This hypothesis is supported by the fact that a wide distribution of pit depths occurs in a single specimen subjected to a nominally uniform environment. In a study of the pit depth distribution evolution in mild steel, Marsh et al.[5] identified four factors having the potential to produce the wide distribution of pit depths observed on any given sample:

1) The pits will have different initiation times;

2) Many pits will cease to propagate following limited growth;

3) The morphology of the pits will vary, with some favoring more rapid mass and charge transfer, and hence faster propagation rates; and

3

4) Some pits will initiate at metallurgical features which may favor more rapid propagation, *e.g.* inclusions and grain boundaries.

Further support for the concept of stochastic pit growth is given by the data and analysis of Aziz[6] for the pitting corrosion of aluminum in tap water. Figure 3 shows the pit depth distribution data of Aziz. When the aluminum is first exposed, a large number of pits initiate and start propagating. After a short time, many pits progressively stifle while only a portion of the population continues to grow, resulting in a backwards "J" shape to the low depth portion of the distribution (This finding supports the concept of permanent pit growth cessation introduced in Section 3.) For those pits still growing, the random influence of the environment on propagation rates results in a bell-shaped distribution, which moves as a body toward greater depths. (This finding directly supports the concept of stochastic pit growth.) After much longer exposures, the mode, *i.e.* peak, of the distribution becomes stationary, and only the deeper pits continue growing. These pits grow at a steadily decreasing rate (which supports the use of a nonlinear increase in pit depth with time, introduced in Section 2.3), and the majority of the pits eventually stifle. These last two findings may result from the build-up of corrosion products within and over pits.
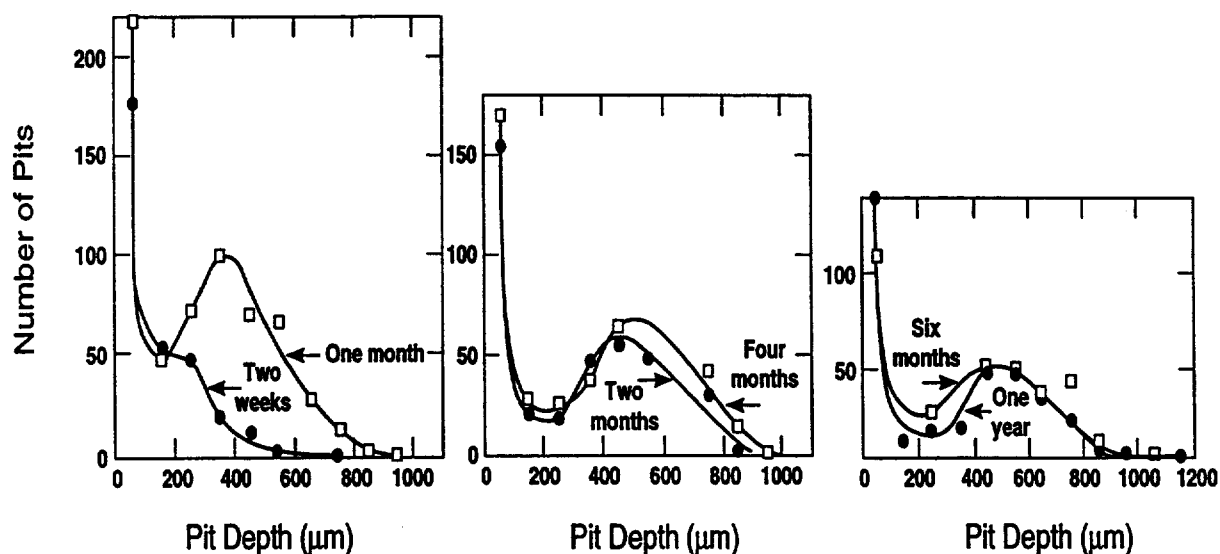

Figure 3. The distribution of pit depths as a function of exposure time for Alcan 2S-O aluminum immersed in tap water. Data of Aziz[6].

2. The Initial Model

2.1 Stochastic pit initiation and growth

Over the past several years, a physically-based, phenomenological, stochastic model of pit initiation and growth has been developed[7-9]. This model is based upon the theory[10] that small fluctuations in the local conditions (*e.g.* electrolyte chemistry, fluid flow rate, surface topography, near-surface microstructure) cause local breakdown of the passive surface film, resulting in the "birth" of metastable pits or "embryos." Many of these embryos become unstable when the local conditions change, and repassivation, or "death," of the embryo results. Once a surviving embryo reaches a critical size or age (the two are assumed to be closely related), it becomes a permanent or "stable" pit and cannot die.

Monte Carlo computer codes have been developed to simulate the stochastic processes of embryo birth and death and the establishment of a stable pit[7]. These codes establish a unit area that is divided into individual "cells" to represent a metal surface in contact with an aggressive environment. During each time step, a random number between 0 and 1 is generated for every cell that does not already contain an embryo or stable pit. If this random number is less than the user-prescribed birth probability, λ, a pit embryo is placed in that cell; otherwise the cell remains empty. Physically, λ corresponds to the probability that, over the area of one cell in a unit time, the local conditions will cause the passive film to break down, thereby initiating a microscopic pit embryo.

For each cell containing an unstable pit embryo, another random number is then generated. If this number is less than the input death probability, μ, the embryo dies and is removed from that cell. The death probability corresponds to the probability that a specific pit embryo, or breakdown in the passive film, will repassivate during a unit time. Pit embryo death has been linked physically, for example, with a reduction in the hydrodynamic boundary layer thickness, which causes a loss of the local concentration excursions needed to support the pit embryo[11].

The "age" of each surviving embryo, *i.e.* the number of time steps it has survived since birth, is incremented at each step and compared with the critical age, τ_c. If the age of an embryo equals τ_c, a stable pit is formed in that cell, which is present for the remainder of the simulation. Physically, the critical age can be related to the ratio of the minimum stable pit depth to the velocity of pit embryo propagation[11]. The minimum stable pit depth is related to the surface roughness and the thickness of the hydrodynamic boundary layer, and the velocity of propagation depends on the electrochemical potential,

aggressive ion concentration, and the nature of the alloy. Finally, note that all three of the pit initiation parameters (λ, μ, τ_c) can be related to experimentally measured quantities[7].

An example of the model predictions for pit initiation is shown in Fig. 4[7]. The parameters used to make this calculation (given in the figure) were chosen arbitrarily, so quantitative agreement with Fig. 2 is not expected. Qualitatively, however, the two distributions are similar, suggesting that the model treats pit initiation in a realistic way. Quantitative comparisons between the model predictions and pit initiation data have been given elsewhere[7] and support the same conclusion.
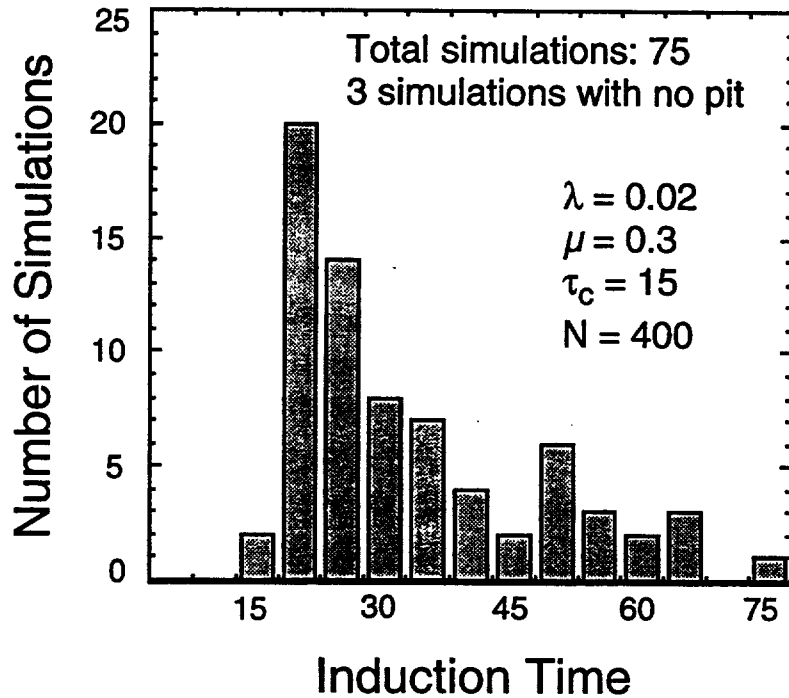
Figure 4. Model predictions of the distribution in stable pit induction times (arbitrary units). Three of the 75 simulations did not produce a stable pit within 75 time steps.

In the initial model, the effects of stochastic stable pit growth on the damage function evolution were included using a simple approach: growth of a stable pit during a particular time step occurs only if a randomly generated number between 0 and 1 is less than the prescribed growth probability, γ. Physically, γ corresponds to the probability that a pit will grow an increment in depth in one unit of time.

An example of the model predictions for stable pit growth under conditions of constant environment is given as a series of histograms in Fig. 5. Each plot gives the number of pits (per unit area) at each depth for a particular exposure time, where time is
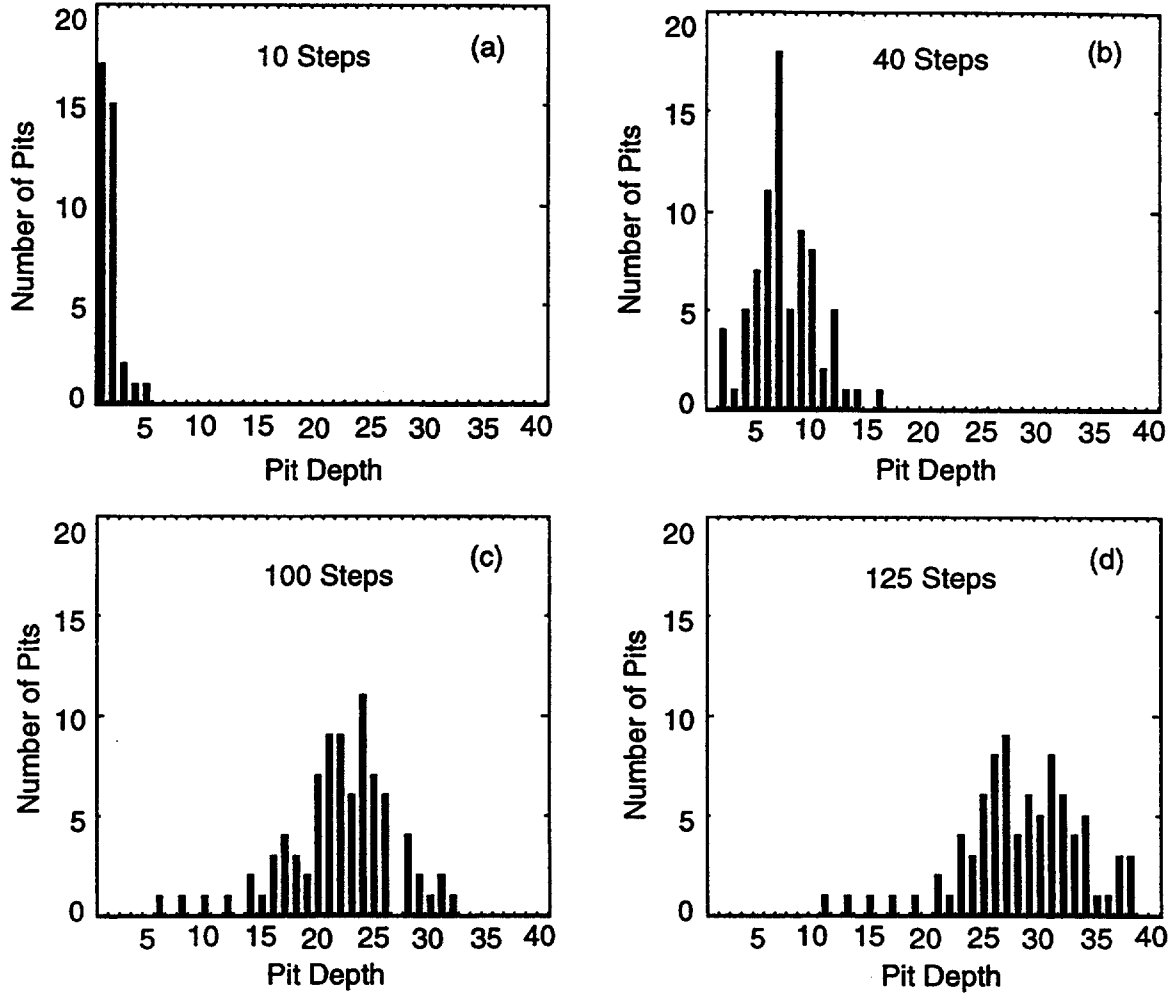
Figure 5. Evolution of the computed damage function histogram for times of (a) 10, (b) 40, (c) 100, and (d) 125 steps. An exponentially decreasing birth probability and a stochastic growth probability of 0.25 were used in the calculations[7]. Pit depths are in arbitrary units.

given in number of time steps, Δt. (As discussed later, quantitative calculations for which exposure times and pit depths have physically meaningful units require experimental data to fit the parameters in the model.) For short times (10 steps) the distribution is narrow, with a large number of pits at low depths. As time increases, the total number of pits increases (40 steps) and the peak in the distribution occurs at an intermediate depth. The number of pits at very low depths is now less than at shorter times. At long times (100, 125 steps), the number of pits stays fairly constant and there are few (if any) pits at low depths. The distribution also begins to broaden, and the number of pits at the peak of the distribution is less than at shorter times. The depth at which the peak occurs increases continuously with time. Many of these gross features are consistent with the data published in the literature, e.g. Fig. 3. However, the linearly increasing maximum pit depth with increasing exposure time and the nearly symmetric shape of the distribution are inconsistent with the available data, as described in Section 2.3.

The utility of damage function evolution predictions like those given in Fig. 5 for purposes of WP container performance assessment (PA) can be demonstrated as follows. Consider the units of pit depth in Fig. 5 to be millimeters, and consider a WP container 32 mm thick. For times of 10 and 40 steps all of the pits have depths less than the thickness of the container, so no release of radionuclides can occur as a result of pitting. Figure 5(c) shows that the time required for first penetration of the container is about 100 Δt, since at this time the first pit with a depth equal to 32 mm has developed. With further exposure to a time of 125 Δt, Fig. 5(d) shows that approximately 25 pits have calculated depths $\geq$ 32 mm, and so will have penetrated a unit area of the container. While the results in Fig. 5 are only qualitative, quantitative predictions could be made by experimentally measuring pit depth distributions over a range of constant environmental conditions, and using the results to provide quantitative values of the model parameters for materials of interest.

2.2 Modeling the effects of environment

One major purpose of modeling pitting corrosion of WP containers is to extrapolate short-time "accelerated" test data to the extremely long service times. Since accelerated testing will require environmental conditions more aggressive than those expected in the repository, these extrapolations will require quantitative predictions of the effects of environment on pit initiation and growth rates. Simulating the effects of environment on pitting also will be required to explore container performance for various environmental scenarios, including the case in which the environment changes with time.

In the context of the stochastic pitting model, the goal is to model the environmental sensitivity of the stochastic parameters: λ, μ, τ_c, and γ. Rigorous development of such relationships has not yet been possible, because it would require considerable experimental work. Therefore, simple but physically reasonable phenomenological expressions have been developed based on a variety of experimental data from the literature. The purpose of this exercise was to provide the means for qualitatively illustrating the potential power of the stochastic approach for predicting the pitting response to various environments. Future efforts should be aimed at improving the physical basis of these expressions, expanding their scope, and quantitatively exploring their predictive capabilities.

Three important environmental parameters have been included in the illustrative model: electrochemical potential, E, chloride ion concentration, [Cl⁻], and absolute temperature, T. Other variables, such as pH, oxygen concentration and the presence of other ions in solution, would need to be included in a complete analysis. Based on a wide variety of published experimental data, the following phenomenological expressions for the environmental dependence of the stochastic parameters were determined[7]:

$$\lambda = A_1 (E - B_1) \cdot \exp(C_1 \cdot [Cl^-]) \cdot \exp(-Q_\lambda / RT) \tag{1}$$

$$\mu = A_2 \cdot \exp(-C_2 \cdot [Cl^-]) \cdot \exp(-Q_\mu / RT) \tag{2}$$

$$\tau_c = A_3 \cdot \exp(-B_3 \cdot E) \cdot \exp(-C_3 \cdot [Cl^-]) \cdot \exp(+Q_\tau / RT) \tag{3}$$

$$\gamma = A_4 (E - B_4)^{B_5} \cdot ([Cl^-])^{C_4} \cdot \exp(+Q_\gamma / RT) \tag{4}$$

where the A's, B's and C's are constants, the Q's are activation energies and R is the gas constant.

Using Eqs. (1)–(4), predictions of the effects of E, [Cl⁻], and T on a variety of pitting phenomena have been made[7,8]. In general, the predictions are qualitatively consistent with published experimental data. Most importantly, it has been demonstrated[7] that this expanded stochastic model can predict the pit depth distribution evolution for continuously changing environmental conditions of the kind actually expected in the repository. Consider the simple, but plausible, environmental scenario shown in Fig. 6[7]. Figure 7 shows the behavior of the stochastic variables computed by Eqs. (1)–(4) for this environmental history. Note how the simple environmental changes can cause complex changes in the stochastic variables, and thus the pitting response.
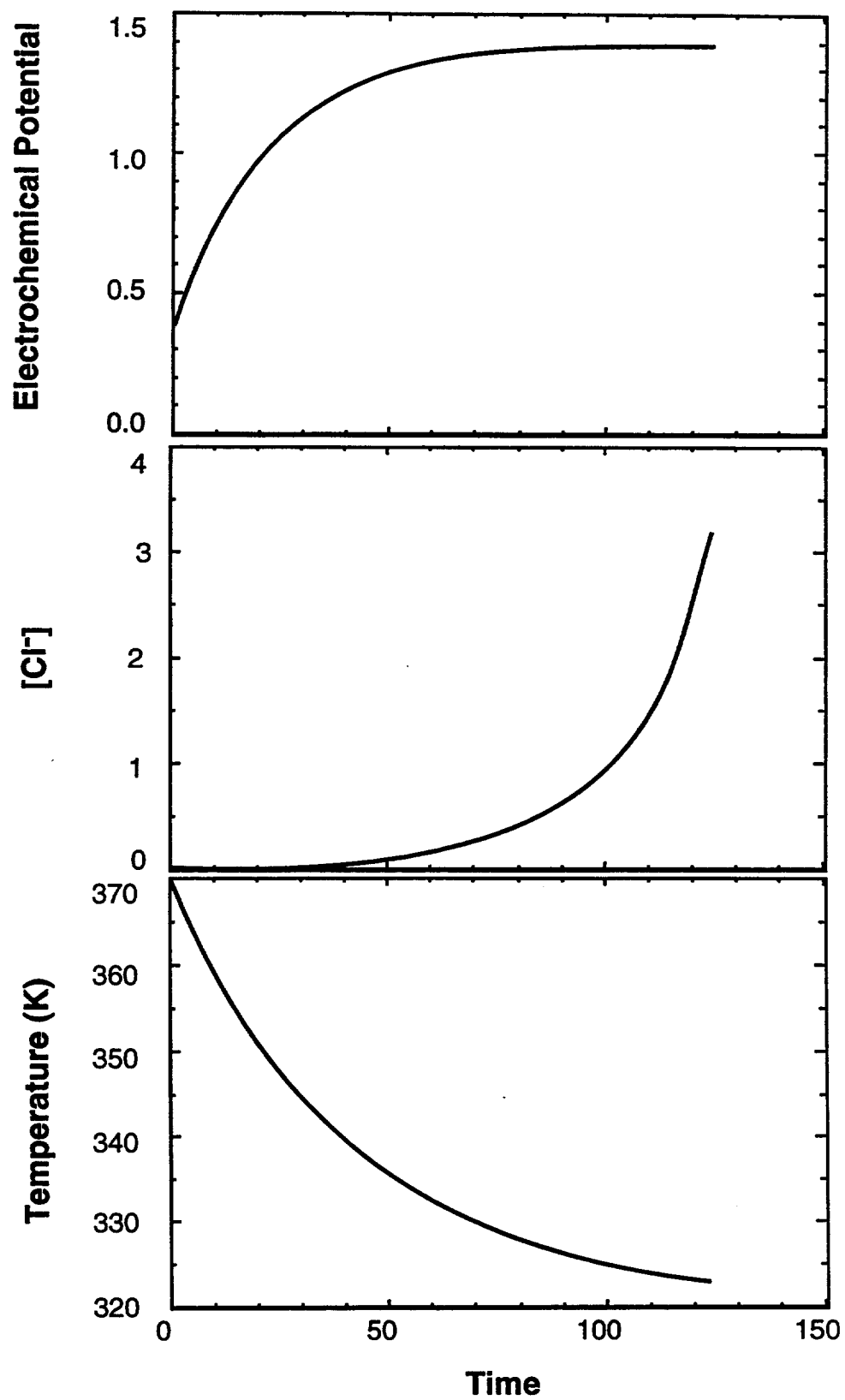
Figure 6. The hypothetical environmental history used to make the predictions given in Figs. 7 and 8. Time, electrochemical potential and chloride ion concentration are in arbitrary units.
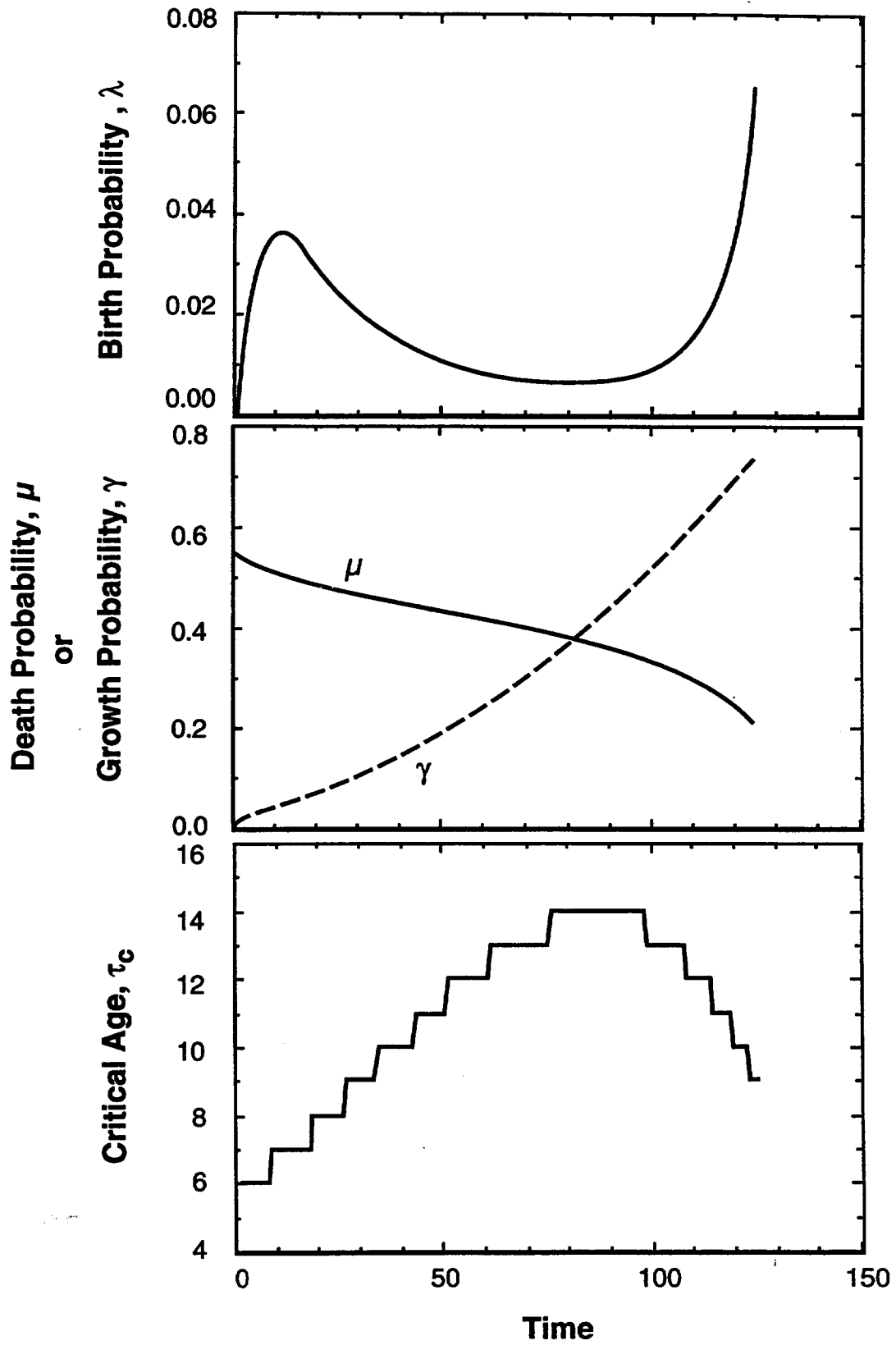
Figure 7. The time dependence of the stochastic parameters resulting from the environmental history given in Fig. 6.

11

This prediction suggests the need for sophisticated models, not just simple empirical laws, to predict the pitting response under realistic conditions. From the time evolution of the stochastic variables, the model can then predict the evolution of the damage function, Fig. 8. Note how the complex environmental history has produced a pit depth distribution after an exposure of 115 steps that has a complex shape compared to the simple shape given in Fig. 5. As described earlier, distributions like those shown in Fig. 8 can be compared with the thickness of the WP container to assess its integrity. Thus, even for complex environmental histories, the model can predict when the container is first breached by a single pit and then how many pits per unit area will breach the container as a function of time for longer exposures. This information then could be used in a more complete PA model to predict radionuclide release rates.

2.3 Deficiencies of the initial model

The pit depth distributions predicted by the initial model for constant environmental conditions, e.g. Fig. 5, properly exhibit an intermediate peak but incorrectly simulate a nearly symmetrical distribution. Data for a wide range of materials and testing conditions reported in the literature[5,6,12-16] show that such distributions actually have a positive skew. In other words, the peak in the distribution occurs toward small pit depths and a relatively long "tail" is exhibited at large depths, e.g. Fig. 3. While this feature of the data may seem to be a minor detail, efforts to more accurately model the tail of the distribution are justified, because the deepest pits are the most significant in terms of WP container degradation.

Related to the lack of a positive skew in the predicted pit depth distributions is the assumption that all stable pits continue to grow, albeit in a stochastic manner, throughout the entire simulation. As discussed in Section 1.2, a variety of data suggest that many small pits cease to grow early during exposure, probably because of a lack of available reactants, such as oxygen and electrons. Further, deep pits may cease to grow later in the exposure because of capping or clogging with corrosion products. The initial model could not simulate such behavior.

Despite the fact that pits grow to have a wide distribution of depths, indicating a probabilistic aspect to pit growth, many theories treat pit growth deterministically, typically as a problem in diffusion[17]. (Of course, the applicability of such theories to millimeter-scale pits is debatable.) These diffusion theories and a variety of experimental observations[6,17] suggest that the pit growth rate decreases as the exposure time and pit depths increase. Equation (5) is often used to phenomenologically describe these deterministic aspects of pit growth (for constant environmental conditions):
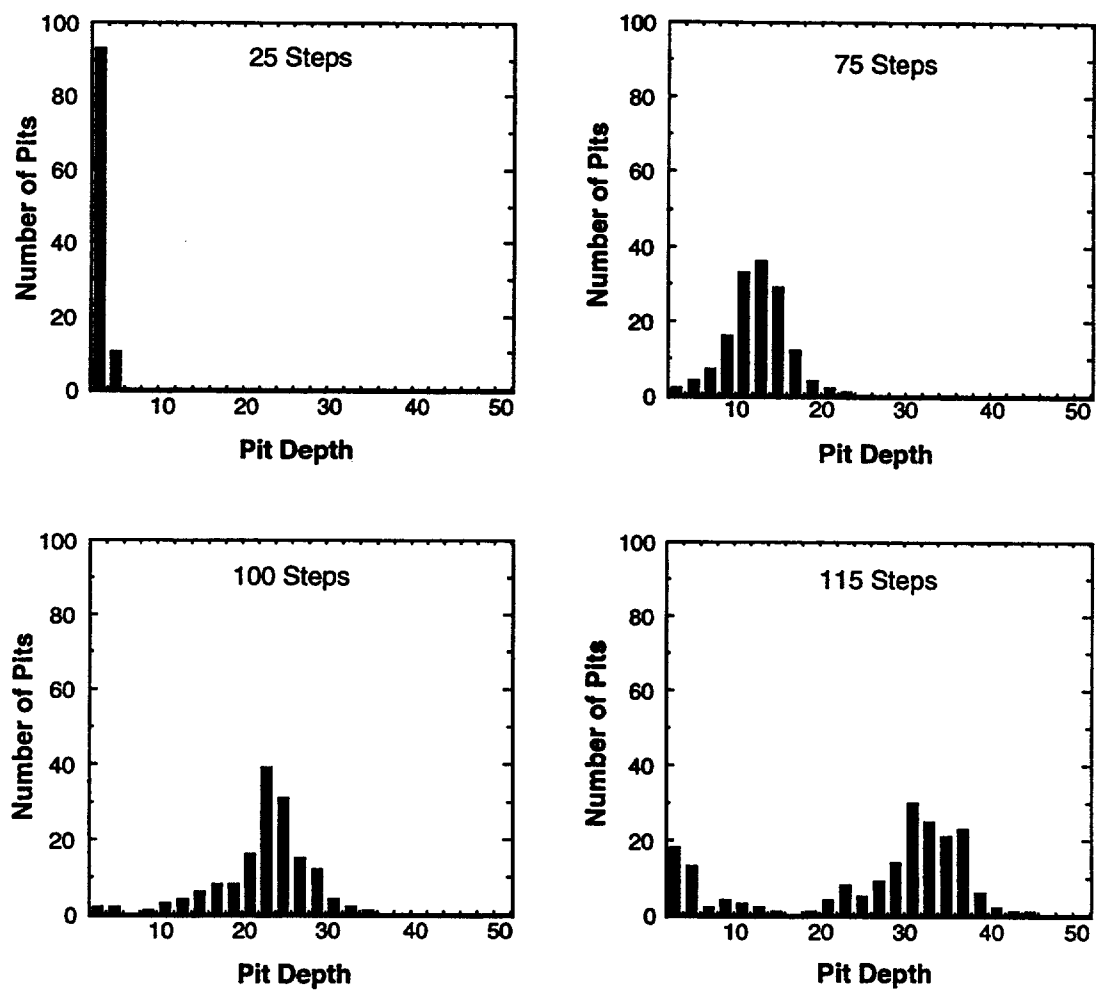
Figure 8. The damage function evolution resulting from the environmental history depicted in Fig. 6. Pit depths are in arbitrary units.

$$d = A t^p , \qquad\qquad (5)$$

where d is pit depth, t is exposure time, and A and p are constants. Typically, $p < 1$, with values of 0.3 and 0.5 being quite common. However, the model presented in Sections 2.1 and 2.2 predicts that the median and maximum pit depth increase linearly with exposure time for constant environmental conditions. This prediction stems from the assumption that the growth probability, γ, is independent of exposure time or pit depth, and the assumption that pit depth is directly proportional to the computed "age" of the pit[9].

Finally, while the physical basis for modeling stochastic pit initiation is solidly based on the theories and experimental results stemming from several careful investigations, the physical underpinnings of the stochastic pit growth model are more tenuous[7,9]. Therefore, it was desirable to improve the link between the pit growth model and accepted physical theories so that model extrapolations of laboratory data can be made with more confidence.

3. The Improved Model

3.1 Changes to the model

As discussed earlier, experimental evidence suggests that many pits cease to propagate following a limited amount of growth. To accommodate this observation, a new stochastic variable was introduced into the model: the probability that during any given time step a stable pit will *permanently* cease to grow, η. Again, a random number between 0 and 1 is generated at each time step for every growing pit, and if this number is less than or equal to η the growth of that pit is permanently halted.

To account for the nonlinear pit depth increase as a function of exposure time discussed in Section 2.3, the phenomenological relationship given in equation (5) was incorporated into the model using two different approaches. The first, or "preliminary," approach to including this deterministic aspect of pit growth involved a straightforward extension of the model described in Section 2.1. The "revised" approach involved a new interpretation of stochastic pit growth and included other changes to make the model more physically realistic.

In the preliminary approach, Eq. (5) was incorporated directly into the model with one slight modification. Instead of representing the exposure time, t is the pit "age," which is less than the actual exposure time for two reasons. First, it takes some "induction" time, τ, to initiate a pit following exposure (Section 2.1). Second, pits are assumed to grow, or "age," stochastically with some probability γ, and may permanently

14

cease to "age" with some probability η; *i.e.* pits do not age during all time steps. Thus, at the end of a simulation the pits have a distribution of "ages," from which the corresponding depths are computed using Eq. (5). Of course, Eq. (5) is not ideal for modeling purposes because it precludes easy treatment of variable environmental histories. However, it was worthwhile to use this equation in combination with the concepts of stochastic pit growth and permanent growth cessation as a means to begin exploring models incorporating both the deterministic and probabilistic aspects of pit growth.

In the revised model, the use of exposure time as an explicit variable to describe a decreasing pit growth rate, Eq. (5), was eliminated. In addition to precluding the easy treatment of variable-environment exposures, the explicit use of exposure time is physically unrealistic since it is the increasing diffusion distance (*i.e.* pit depth), not exposure time *per se*, that causes the decrease in pit growth rate. The revised model also employs a new approach for simulating the stochastic aspects of pit growth. This approach was motivated by the interpretation of experimental pit depth distribution data by Marsh *et al.*[5]. These investigators suggested that the stochastic variation in pit growth rates stems from the variations in pit morphology and local metallurgical conditions, which cause variations in the charge and mass transfer rates from pit to pit. Thus, pits grow continuously but at a variety of rates. The permanent pit growth cessation probability, η, also was included in the revised model.

To incorporate these two new concepts of stochastic pit growth into the model, Eq. (5) can be modified as follows:

$$^k d = {}^k A \, (t - {}^k \tau)^p \; ; p < 1, \tag{6}$$

where in this case t is the actual exposure time and the superscript k is used to distinguish among all the individual pits in the simulation. Note that each pit has its own induction time, $^k\tau$, and its own value of A. The stochastic variation in pit growth rates is simulated by randomly assigning a specific value of $^k A$ for each pit from a prescribed, possibly nonuniform, distribution. In the analysis performed here, it is assumed that the values of $^k A$ are distributed according to a normal, or Gaussian, distribution. Taking the time derivative of Eq. (6) and substituting for the quantity $(t - {}^k\tau)$ by inverting Eq. (6) gives an equation for the rate of pit growth that depends only on the depth of the pit, and not on the exposure time. Writing this equation in incremental form with Δt as the time step size gives the following:

$$\frac{\Delta^k d}{\Delta t} = p\left(^kA\right)^{1/p}\left(^kd\right)^{p-1/p} , \tag{7}$$

where

$$\Delta^k d = {}^kd_i - {}^kd_{i-1} , \tag{8}$$

and the subscript i denotes the current time step. Thus, at any time step i in the simulation, the increment in pit growth can be written as a function only of the time step size, the pit depth at the previous time step, and the constants ^kA and p:

$$^kd_i = {}^kd_{i-1} + \Delta t\left[p\left(^kA\right)^{1/p}\left(^kd_{i-1}\right)^{p-1/p}\right] . \tag{9}$$

Calculations have shown that the pit depth distributions predicted using Eq. (9) are independent of time step size if the proper modifications are made to the input probabilities (e.g., λ, μ, η) to account for a change in Δt [7].

To implement Eq. (9), a method was established for producing random values of ^kA from a population that is normally distributed. An algorithm was identified[18,19] that produces random values from the standard normal distribution using a uniform random number generator, such as the one already implemented in the initial Monte Carlo code. Thus, for any value taken randomly from the standard normal distribution, Z, the value of ^kA with the corresponding cumulative probability is simply:

$$^kA = \sigma Z + \mu , \tag{10}$$

where σ and μ are the standard deviation and mean of the desired ^kA distribution, which are input prior to the simulation.

3.2 Model predictions

Figure 9 illustrates the capability of the new model in its preliminary form to simulate the complex time evolution of the pit depth distribution. For this simulation, the probability of initiating a new pit embryo was decreased exponentially with exposure time[7] such that no new pits were initiated for exposures greater than approximately 50 time steps. The parameters affecting the growth of these pits, γ, η, A and p, were chosen arbitrarily and are given in the figure. Following 100 time steps, Fig. 9(a), the

16

distribution exhibits a peak at the lowest depths, followed by a decrease in the number of pits with increasing depth, and then a second local maximum. This gives the backwards "J" shape to the initial part of the distribution noted by Aziz (Fig. 3). Experimentally, this portion of the distribution was attributed to the stifling of shallow pits. In the model, this same feature is caused by the permanent cessation of growth for many small pits through the parameter η. As the exposure time increases, the heights of the two peaks decrease somewhat as the distribution broadens, Fig. 9(b). The broad distribution of pit depths, particularly beyond the backwards "J" feature, was attributed by Aziz[6] largely to the randomly varying propagation rates for individual pits. This same characteristic is predicted by the preliminary model largely through the stochastic growth probability, γ. With further increases in exposure time, the two peaks remain stationary and only the deepest pits continue to grow, creating a long "tail" to the distribution, Fig. 9(c). This same feature in the data of Aziz, Fig. 3, is caused by the eventual stifling of most pits, so that only a few grow to large depths. Consistent with this finding, the growth cessation probability, η, causes most pits to stop growing after 500 time steps. Finally, note in Fig. 3 that the maximum pit depth, d_{max}, increases ever more slowly as the exposure time increases. A similar phenomenon is evident in Fig. 9. Following 100 time steps $d_{max} = 3.5$, while after a five-fold increase in exposure time d_{max} has less than doubled to 5.5, Fig. 9(c). This prediction results partly from the use of Eq. (5) with $p = 0.5$. In addition, the rate of increase for d_{max} slows due to the use of $\eta = 0.01$. Consider that for an exposure of 500 steps only four of the initial 590 pits are still growing. This implies that the pits which early in the exposure were of maximum depth probably have permanently halted, requiring shallower pits to grow and become the deepest active pits at longer exposures. In summary, the complex pit depth distribution evolution exhibited in Fig. 3 is qualitatively predicted by the new preliminary model through the consideration of both the stochastic and deterministic aspects of pit growth.
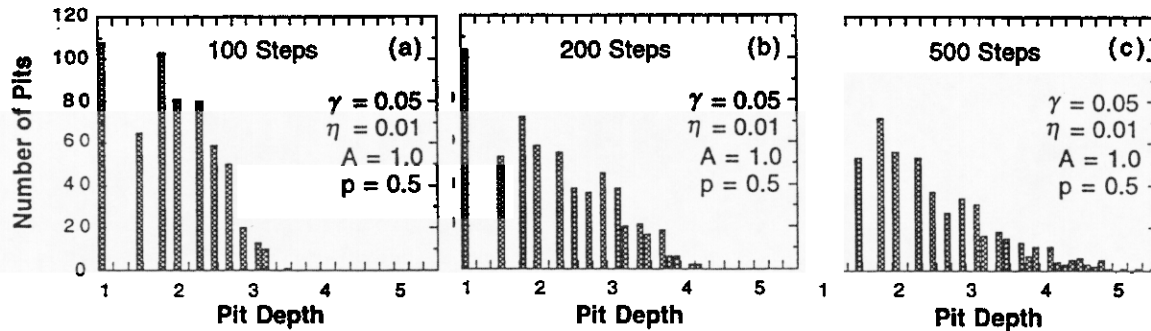

Figure 9. Distribution in pit depths computed by the preliminary model for the growth parameters given in the figure and exposures of: (a) 100 time steps, (b) 200 time steps, and (c) 500 time steps. Pit depths are in arbitrary units.

Of course, the evolution of the pit depth distribution is sensitive to the input parameters affecting pit growth. Calculations have shown that the shapes of the distributions during various stages of evolution are most sensitive to the relative values of the pit growth and cessation probabilities, γ and η. Experimental measurements of the pit depth distribution evolution for materials and environments of interest would be required to quantitatively determine values of γ, η, and the other model parameters.

Figure 10 presents the results of calculations similar to those shown in Fig. 9 but performed using the revised model. A permanent pit growth cessation probability of $\eta = 0.01$ and a time exponent of $p = 0.5$ again were used in these simulations. For relatively short exposure times, e.g. 50 time steps, Fig. 10(a) shows that the distribution of pit depths is nearly symmetric. In the revised model, this distribution in pit depths is largely caused by the distribution in A values, Eq. (10), since each active pit grows during every time step. Note that the backward "J" shape of the distribution at small pit depths present in the data of Aziz[6] and in the calculations presented in Fig. 9 is absent in Fig. 10. Fortunately, this aspect of the distribution has little practical importance because these pits are small and don't grow. For intermediate exposures, Fig. 10(b) shows that much of the distribution moves as a body toward larger pit depths so that the distribution remains roughly "bell" shaped. However, it becomes somewhat skewed toward small pit depths with an increasingly long tail at large depths. Similar features are observed in the data given in Fig. 3 for pits beyond the backward "J." Finally, for relatively long exposures, Fig. 10(c) shows that the distribution has become nearly stationary, with only the deepest pits continuing to grow, making the tail at large depths more extensive. Again, this feature of the predictions is qualitatively consistent with that computed by the preliminary model and observed experimentally, Fig. 3.
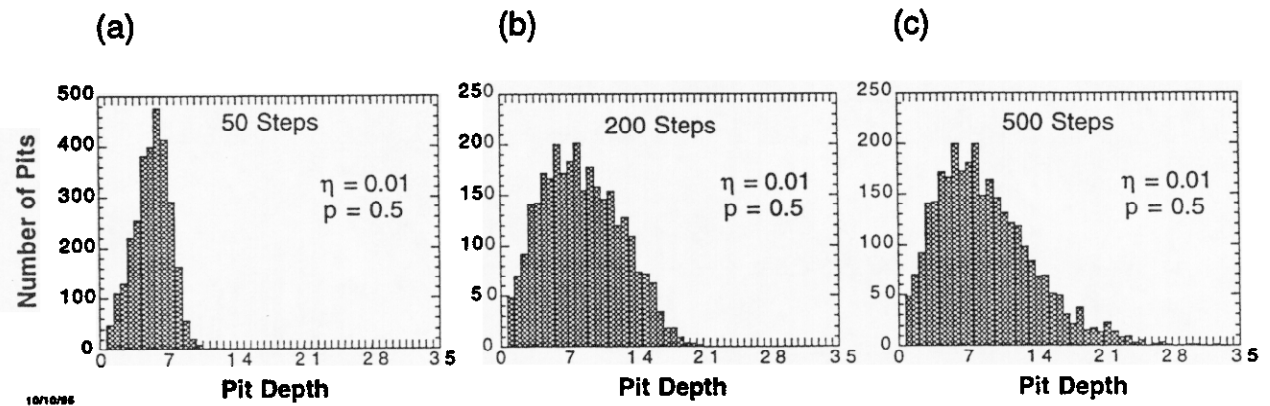

Figure 10. Distribution in pit depths computed by the revised model for the growth parameters given in the figure and exposures of: (a) 50 time steps, (b) 200 time steps, and (c) 500 time steps. Pit depths are in arbitrary units.

The new model, both in its preliminary and revised forms, is capable of simulating the nonlinear dependence of the maximum pit depth on exposure time (for constant environmental conditions). Figure 11 shows an example for the revised formulation using input values of $p = 0.5$ and $\eta = 0.001$. The plot with linear axes, Fig. 11(a), emphasizes the striking decrease in the pit growth rate with increasing exposure time and pit depth. The logarithmic plot in Fig. 11(b) shows that, as expected, the predicted time exponent equals the input value of p, so long as significant permanent pit growth cessation has not occurred. This latter phenomenon is what causes the computed maximum pit depth at 5000 steps to be somewhat below the line for $p = 0.5$.

In summary, the new model is capable of qualitatively reproducing the shapes of the pit depth distributions typically observed experimentally, including the presence of a long tail at large depths. The new model also predicts a nonlinear increase in maximum pit depth with increasing exposure time, consistent with a wide variety of data. These improvements stem from a combination of changes related to the stochastic and deterministic aspects of pit growth. Minor differences exist between the preliminary and revised versions of the new model in the details of their predictions regarding pitting damage (also see Section 4). However, neither method is clearly superior to the other in the accuracy of its predictions, though the revised model has a stronger physical basis. Experimental data relevant to modeling pitting corrosion of WP containers are required to make a final judgment regarding the suitability of the two methods.

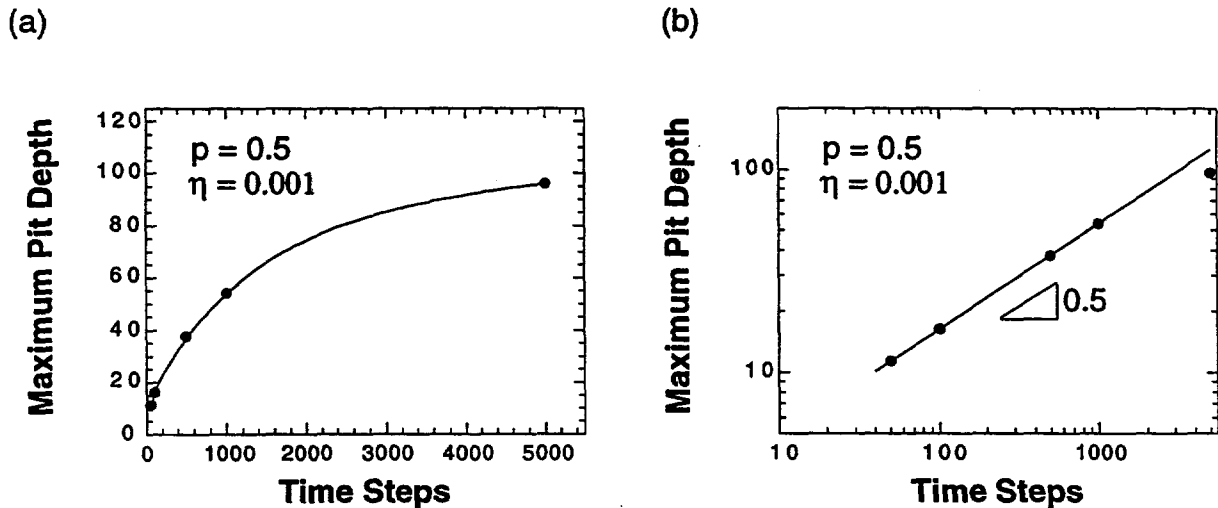(a)   (b)

Figure 11. Revised model predictions of the time dependence of the maximum pit depth are plotted on (a) linear and (b) double-logarithmic axes. Pit depths are in arbitrary units.

4. Dependence of Maximum Pit Depth on Surface Area Exposed

The method of "extreme-value statistics" (EVS) is commonly employed in the analysis of experimental pit depth data[6,12-14]. EVS is particularly valuable for predicting the commonly observed logarithmic increase in maximum pit depth with increasing specimen or service component surface area[5,6,14,15]. In the context of WP container design and performance assessment, EVS analysis of laboratory data collected on a limited number of small specimens might provide the means to predict the probability of pits reaching significant depths (*e.g.* equal to the container thickness) over the surface of an entire container, or many containers. Such a prediction should be accurate so long as the extrapolated maximum pit depth exceeds the deepest measured pit by no more than about a factor of three[6]. Fortunately, this provides an extrapolation in exposed surface area of up to three orders of magnitude.

Given the utility and wide acceptance of EVS to analyze pitting damage, it is useful to determine if the stochastic pitting model is consistent with this method. Therefore, modifications to the Monte Carlo code were made which follow from the actual experimental procedure described by Aziz[6]. First, an individual test coupon is simulated by a single model "run" using a unique "seed" value to initiate the random number generator[7]. Using a single set of input parameters, an *N*-run simulation is performed in which each run begins with a different random number seed. This procedure corresponds to the exposure of multiple, identical test coupons to the same corrosive environment, as described by Aziz[6]. Analogous to the experiments, the surface area simulated is proportional to the number of runs in the simulation, since one run represents a unit surface area. Following each run within a particular *N*-run simulation, the maximum computed pit depth is stored. Once all *N* runs have been completed, these values are sorted in ascending order, providing "data" analogous to those collected experimentally[6]:

$$d_1^{max} \leq d_2^{max} \leq ... \leq d_m^{max} \leq ... \leq d_N^{max} . \tag{11}$$

The cumulative probability that the deepest pit is less than or equal to d_m^{max} is then computed from these data as:

$$\Phi_m = m / (N + 1). \tag{12}$$

These probabilities from the Monte Carlo simulation are then analyzed using the most common expression for the expected extreme-value distribution[6]:

$$\Phi_m = \exp\left[-\exp\left(-y_m\right)\right],\tag{13}$$

where y_m is the "reduced variate." The reduced variate is defined as:

$$y_m = \alpha\left(d_m^{max} - u\right),\tag{14}$$

where u is the "mode" (highest point of the extreme-value distribution) and α is the "scale" parameter measuring the width of this distribution. The values of u and α are fit to the Monte Carlo "data," Eq. (11), as follows. First, Eq. (13) is solved for y_m, giving:

$$y_m = -\ln\left\{-\ln\left(\Phi_m\right)\right\},\tag{15}$$

where Φ_m is computed from the Monte Carlo results using Eq. (12). For each value of Φ_m, a corresponding y_m is computed from Eq. (15). Then, the data pairs (d_m^{max}, y_m) are plotted on linear axes and fit to Eq. (14) using linear least squares analysis to determine α and u. Extrapolation of this fitted line provides predictions of the probability and exposure time required for the occurrence of a pit of any given depth[6].

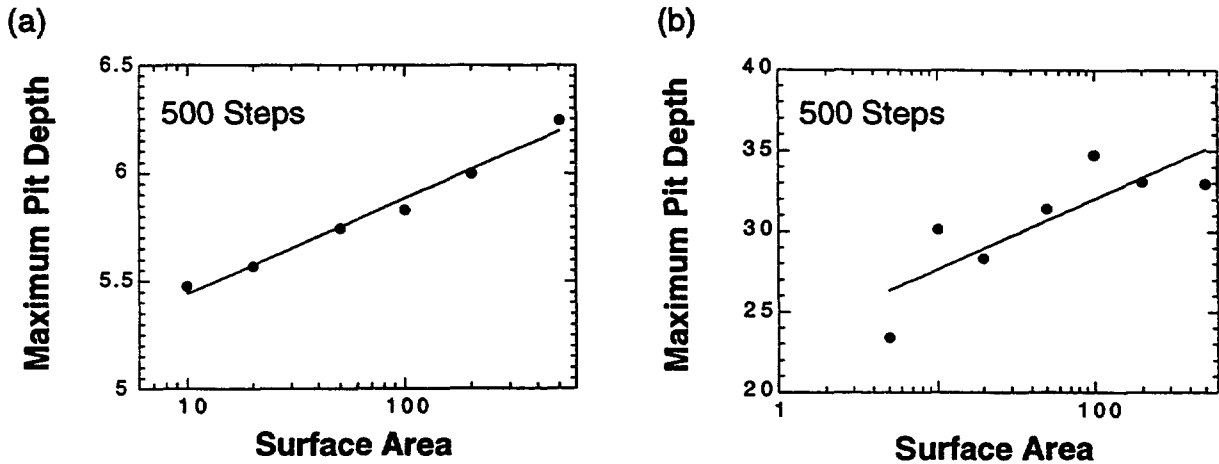(a)   (b)

Figure 12. Predictions of the increase in maximum pit depth with increasing exposed surface area from (a) the preliminary model, and (b) the revised model. Pit depth and surface area are in arbitrary units.

21

In general, the stochastic model is consistent with the EVS theory. For example, it has been shown[9] that the d_m^{max} vs y_m plots predicted by the stochastic model are qualitatively consistent with those measured experimentally in several material-environment systems[6,12-14]. Most importantly, consistent with previous EVS analyses and data, the stochastic model predicts that the maximum pit depth increases logarithmically with increasing exposed surface area, Fig. 12. Thus, by performing simulations with identical input parameters and varying the numbers of runs, the effect of exposed container surface area on the maximum pit depth can be predicted by the stochastic model.

5. Experimental Validation

Modeling cannot progress without input from experimental data. Experimental data are required to fit the model parameters so that quantitative predictions can be made, to verify the accuracy of the model, to validate the basic model assumptions, and if necessary to re-formulate the model. Ideally, the process of modeling and testing is iterative, with these efforts taking place in parallel so that results from one can drive improvements in the other. Plans for experimental support of the stochastic modeling effort have been made[20-22] but funding constraints have limited the execution of these plans.

To date, the experimental validation of the models has been limited to a few preliminary measurements of the pit depth distribution evolution in Incoloy 825. Briefly, these experiments involve exposing flat specimens to an aggressive aqueous environment. A constant electrochemical potential is applied to the specimens to induce relatively rapid pitting under controlled conditions. Each specimen is removed from the aggressive environment following a prescribed exposure time, and is examined to measure the distribution of pit depths. The evolution of the distribution with increasing exposure time can then be compared with model predictions to test the assumptions and equations used in the model.

Specifically, potentiostatic polarization experiments were performed on 1 cm^2 samples of Incoloy 825 immersed at 90 °C in 5% NaCl aqueous solution containing sulfuric acid (pH ≈ 2.6). Using optical microscopy, the depth of each pit was measured by calibrated focusing, and the pit diameters were measured with a filar eyepiece. (Note that pits with depths less than about 25 µm, of which there were many, were not measured). Examples of the measured pit depth and diameter distributions are given in Fig. 13. These distributions are qualitatively similar to the predicted distributions shown

in Fig. 10 for relatively short exposures. In particular, there is a peak in the distributions at an intermediate depth or diameter. However, the long tail in the distribution at large depths (or diameters) that is predicted by the model for long exposures is not observed in the short-exposure distributions given in Fig. 13. Longer time exposures are required to test this prediction of the model. Table 1 gives a summary of the measured pit depth data gathered to date. Although these data are insufficient to draw many firm conclusions, it appears that increasing the applied electrochemical potential, E_{app}, increases the number of pits per unit area. The effects of exposure time and electrochemical potential on pit depths are not yet clear.
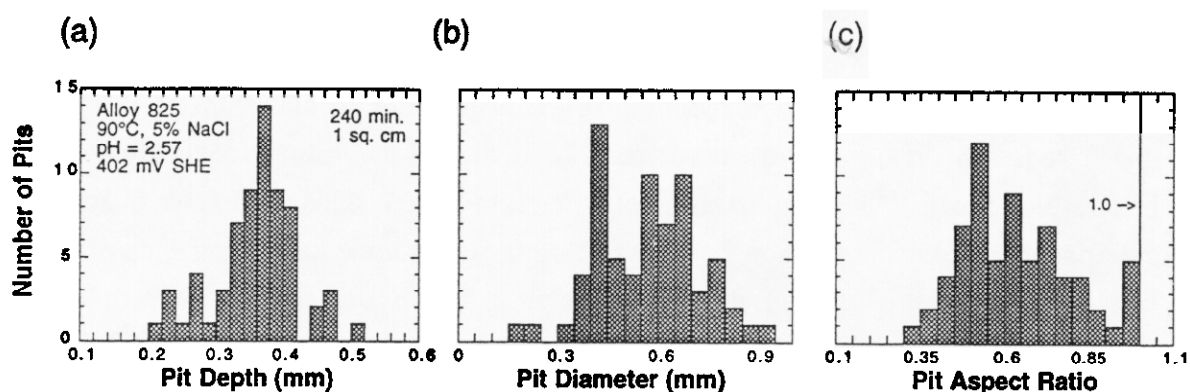

Figure 13. Experimental distributions of (a) pit depth, (b) diameter, and (c) aspect ratio for Incoloy 825 immersed for 240 minutes at 90 °C in pH 2.57, 5% NaCl solution and polarized at 402 mV SHE. Unpublished data of Henshall and Roy [23].

Table 1. Pit depth distribution data for 1 cm^2 samples of Incoloy 825 immersed in acidified brine (5% NaCl) at 90 °C. Data of Henshall and Roy [23].

E_{app} (mV SHE)	Exposure Time (min.)	pH	Number of Pits	Maximum Depth (mm)	Median Depth (mm)
372	480	2.67	1	0.361	0.361
382	120	2.66	6	0.653	0.449
382	232	2.64	34	0.899	0.621
392	218	2.51	21	0.822	0.681
402	240	2.57	68	0.505	0.363

Figure 13(c) shows the distribution in pit aspect ratios, defined as the pit depth divided by the diameter. If the aspect ratio is less than one (broad, shallow pits),

automated pit depth measurement techniques may be viable for future work, or the pit diameter could be used as a conservative measure of damage. The data given in Fig. 13(c) reveal that all pits have an aspect ratio less than one for this experiment, though testing under somewhat different conditions revealed aspect ratios of up to 2. Again, more data are required to make a firm conclusion regarding pit aspect ratios in Alloy 825.

6. Summary and Conclusions

A phenomenological, stochastic model of pit initiation and growth has been developed in support of waste package container design and performance assessment. This model can simulate the time evolution of the distribution in pit depths on a metal surface exposed to an aggressive environment. A review of the initial model revealed it to be capable of realistically simulating stochastic pit initiation. This model also includes simple phenomenological relationships describing the environmental dependence of the stochastic parameters. Therefore, it can simulate pit initiation and growth under variable-environment histories, such as those anticipated in the repository.

Recent improvements to this model have focused on pit growth and the time evolution of the pit depth distribution. These improvements include the capability to model permanent pit growth cessation, methods to deterministically predict a nonlinear increase in maximum pit depth with increasing exposure time (for constant environmental conditions), and a more physically realistic treatment of stochastic pit growth. These improvements have resulted in predictions that are qualitatively more consistent with a variety of experimental data in the literature, for example the development of pit depth distributions with a positive skew and a long tail at large pit depths. Further, this model has been shown to be consistent with extreme-value statistical methods for predicting the logarithmic increase of maximum pit depth with increasing exposed surface area.

A critical need has been identified for generating experimental data for candidate container materials exposed to repository-relevant environments. These data are required to quantitatively assess and further develop the model. Preliminary pit depth distribution data for Incoloy 825 have been presented. These data are qualitatively consistent with stochastic model predictions of a peak in the pit depth distribution at intermediate depths, and show that this alloy is susceptible to pitting under aggressive conditions.

Acknowledgments

References

1. H. Fontana and N. Greene, "Corrosion Engineering," 2nd Edition, McGraw-Hill, pp. 39-57 (1967).

2. D. Shoesmith, "Modelling to Predict the Corrosion Behavior of Nuclear Waste Containers," presented at the *Forum for the Use of Nickel Alloys for Radwaste Containers*, Tucson, AZ, Feb. 22-23 (1995).

3. R. W. Andrews, "TSPA-95 Objectives and Approach: Focus on Waste Packages/EBS Conceptual Models," presented at the NWTRB Full Board Meeting, Las Vegas, NV, Apr. 19-20, (1995).

4. T. Shibata and T. Takeyama, "Stochastic Theory of Pitting Corrosion," *Corr.* 33 (1977) 243-251.

5. G. P. Marsh, I. D. Bland, and K. J. Taylor, "Statistical Study of Pit Propagation in Carbon Steel Under Nuclear Waste Disposal Conditions," *Br. Corros. J.* 23, 157-164 (1988).

6. P. M. Aziz, "Application of the Statistical Theory of Extreme Values to the Analysis of Maximum Pit Depth Data for Aluminum," *Corros.* 12, 495-506 (1956).

7. G. A. Henshall, "Modeling Pitting Corrosion Damage of High-Level Nuclear-Waste Containers using a Stochastic Approach," *J. Nucl. Mater.* 195, 109 (1992).

8. G. A. Henshall, "Stochastic Modeling of the Influence of Environment on Pitting Corrosion Damage of Radioactive-Waste Containers," in *Scientific Basis for Nuclear Waste Management: XVIII,* T. Murakami and R.C. Ewing, eds., MRS, Pittsburgh, PA, p. 679-686 (1995).

9. G. A. Henshall, "A Phenomenological Approach to Simulating the Evolution of Radioactive-Waste Container Damage Due to Pitting Corrosion," in *Scientific Basis for Nuclear Waste Management: XIX,* W. M. Murphy and D. A. Knecht, eds., MRS, Pittsburgh, PA, pp. 613-619 (1996).

10. D. E. Williams, C. Westcott and M. Fleischmann, "Stochastic Models of Pitting Corrosion of Stainless Steels: I. Modeling of the Initiation and Growth of Pits at Constant Potential," *J. Electrochem. Soc.* **132**, 1796-1804 (1985).

11. D. E. Williams, C. Westcott and M. Fleischmann, "Stochastic Models of Pitting Corrosion of Stainless Steels: II. Measurement and Interpretation of Data at Constant Potential," *J. Electrochem. Soc.* **132**, 1804-1811 (1985).

12. J. E. Strutt, J. R. Nicholls, and B. Barbier, "The Prediction of Corrosion by Statistical Analysis of Corrosion Profiles," *Corros. Sci.* **25**, 305-315 (1985).

13. H. F. Finley, "An Extreme-Value Statistical Analysis of Maximum Pit Depths and Time to First Perforation," *Corros.* **23**, 83-87 (1967).

14. G. G. Eldredge, "Analysis of Corrosion Pitting by Extreme-Value Statistics and its Application to Oil Well Tubing Caliper Surveys," *Corros.* **13**, 51-60 (1957).

15. J. W. Provan and E. S. Rodriguez, "Part I: Development of a Markov Description of Pitting Corrosion," *Corros.* **45**, 178-192 (1989).

16. V. Y Flaks, "Statistical Model of Size Distribution of Pittings During Atmospheric Corrosion of Aluminum Alloys," *Protection of Metals*, **9**, 407-409 (1973).

17. A. Hoch, A. Honda, H. Ishikawa, F. Porter, S. Sharland and N. Taniguchi, "A Modelling and Experimental Study for Long-Term Prediction of Localised Corrosion in Carbon Steel Overpacks for High-Level Radioactive Waste," in *MRS Symposium on the Scientific Basis for Nuclear Waste Management XVIII*, pp. 703-710 (1995).

18. W. H. Press, B. P. Flannery, S. A. Teukolsky and W. T. Vetterling, *Numerical Recipes: The Art of Scientific Computing*, Cambridge Univ. Press, Cambridge, pp. 202-203 (1986).

19. G. E. Forsythe, M. A. Malcom, and C. B. Moler, *Computer Methods for Mathematical Computations*, Prentice-Hall, New Jersey, p. 247 (1977).

20. G. A. Henshall, "Modeling and Experimental Investigations of Pitting Corrosion in High-Level Radioactive-Waste Container Materials," January 13, 1995. An informal report presented to LLNL-YMP management.

21. G. A. Henshall, A. K. Roy, and D. Jones, "Preliminary Experimental Program to Support the Stochastic Pitting Modeling Effort – I. Pit Initiation," June 13, 1995. An informal proposal presented to LLNL-YMP management.

22. G. A. Henshall and A. K. Roy, "Preliminary Experimental Program to Support the Stochastic Pitting Modeling Effort – II. Pit Growth," June 28, 1995. An informal proposal presented to LLNL-YMP management.

23. G. A. Henshall and A. K. Roy, Lawrence Livermore National Laboratory, unpublished data (1996).